Hybrid Palladium Nanoparticles for Direct Hydrogen Peroxide Synthesis: The Key Role of the Ligand

Journal Article

Author(s):
Lari, Giacomo M.; Puértolas, Begoña; Shahrokhi, Masoud; López, Núria; Pérez-Ramírez, Javier

Publication date:
2017-02-06

Originally published in:
Angewandte Chemie. International Edition 56(7), https://doi.org/10.1002/anie.201610552

Hybrid Palladium Nanoparticles for Direct H_2O_2 Synthesis: the Key Role of the Ligand

Giacomo M. Lari[+][a], Begoña Puértolas[+][a], Masoud Shahrokhi[b], Núria López[b], and Javier Pérez-Ramírez*[a]

Abstract: Ligand-stabilized palladium nanoparticles deposited on a carbon carrier efficiently catalyze the direct synthesis of H_2O_2 and the unique performance is due to their hybrid nanostructure. Catalytic testing demonstrated that the selectivity increases with the HHDMA ligand content from 10% for naked nanoparticles up to 80%, rivalling that obtained with state-of-the-art bi-metallic catalysts. Furthermore, it remains stable over five consecutive reaction runs owing to the high resistance towards leaching of the organic moiety, arising from its covalent bond with the metal surface. As rationalized *via* Density Functional Theory, this behavior is attributed to the adsorption mode of the reaction intermediates on the metal surface. Whereas they lie flat in the absence of the organic shell, their electrostatic interaction with the ligand result in a unique vertical configuration which prevents further dissociation and overhydrogenation. These findings not only have strong practical relevance for the industrial implementation of the process, but also show the importance of understanding the substrate-ligand interaction to develop smart hybrid catalysts.

Hydrogen peroxide, H_2O_2, attracts growing attention as a green alternative to traditional stoichiometric oxidants in a wide range of applications within the textile, pulp bleaching, waste water treatment, metallurgy, cosmetic, and pharmaceutical industries. Owing to the advantages of its use, *i.e.* the high atom economy and the generation of water as the only byproduct,[1] an increase of its global market value from 3.7 to 6.0 billion USD between 2014 and 2023 is forecasted.[2] Nowadays, the production of H_2O_2 relies exclusively on the anthraquinone process, which, despite being safe and suitable for continuous operation, involves the use of quinones and solvents resulting in energy-intensive purification steps and the generation of vast amounts of waste, thus being competitive only at large scale.[1,3] The direct synthesis of H_2O_2 is an appealing alternative that has the potential to be exploited in decentralized plants at any scale due to the (i) absence of organic substrates, (ii) utilization of green solvents such as water or methanol, and (iii) simplified purification.[1,4] Its applicability has been widely investigated as such or in tandem with selective oxidation reactions using heterogeneous or, seldom, homogeneous catalysts.[5] Albeit the number of advantages over the traditional route, its industrial implementation has been hindered by the low selectivity of the most active catalyst identified, *i.e.* supported Pd nanoparticles (NPs).[6] Indeed, besides facilitating the reaction between molecularly adsorbed O_2 and H atoms, Pd NPs favor O_2 dissociation leading to undesired water formation (**Scheme 1**).[7] To overcome this limitation, the addition of a second metal, chiefly Au or Sn, which was shown to generate active sites that prevent O-O bond cleavage, resulted in the most selective catalysts reported to date.[8] Still, the added loading of costly and/or toxic metals hampers their widespread utilization.

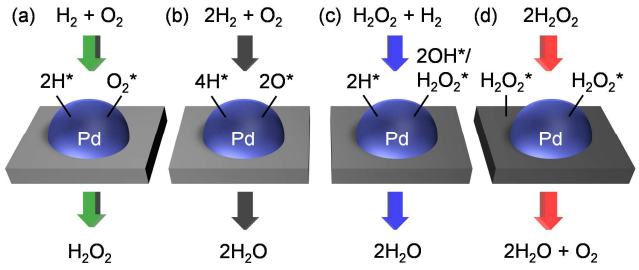

Scheme 1. Reactants, products, and relevant adsorbed intermediates in the (a) direct synthesis of H_2O_2 and the side reactions leading to water formation *via* (b) unselective O_2 hydrogenation, (c) H_2O_2 hydrogenation, and (d) H_2O_2 decomposition over supported Pd catalysts.

In our quest to develop a superior catalyst, we were attracted by nanostructured hybrid materials, incorporating active metal NPs covered by an adsorbed layer of large organic molecules, such as polymers or surfactants.[9] The latter not only prevent the aggregation of the active phase, but were also demonstrated to boost the selectivity in the stereospecific hydrogenation of carbonyl groups, the partial hydrogenation of alkynes, nitroaromatics, and unsaturated epoxides, and the alcoholysis of silanes owing to the blockage of unselective facets, the modification of the adsorption energies of reactants, intermediates, and products, the precise control of surface structures, or the interfacial electronic effect.[10] Despite these encouraging results, they remain overlooked in the context of direct H_2O_2 synthesis, where only poly-vinyl alcohol (PVA)-capped Pd particles were recently suggested to limit O_2 dissociation.[11] Although the initial H_2O_2 selectivity was notable (*ca.* 95%), it rapidly decreased due to leaching of the organic

[a] G. M. Lari,[+] Dr. B. Puértolas,[+] Prof. Dr. J. Pérez-Ramírez
Institute for Chemical and Bioengineering
Department of Chemistry and Applied Biosciences
ETH Zurich
Vladimir-Prelog-Weg 1, 8093 Zurich (Switzerland)
E-mail: jpr@chem.ethz.ch

[b] Dr. M. Shahrokhi, Prof. Dr. N. López
Institute of Chemical Research of Catalonia (ICIQ) and Barcelona Institute of Technology
Av. Països Catalans 16, 43007 Tarragona (Spain)

[+] Equal contribution.

Supporting information for this article is given via a link at the end of the document.

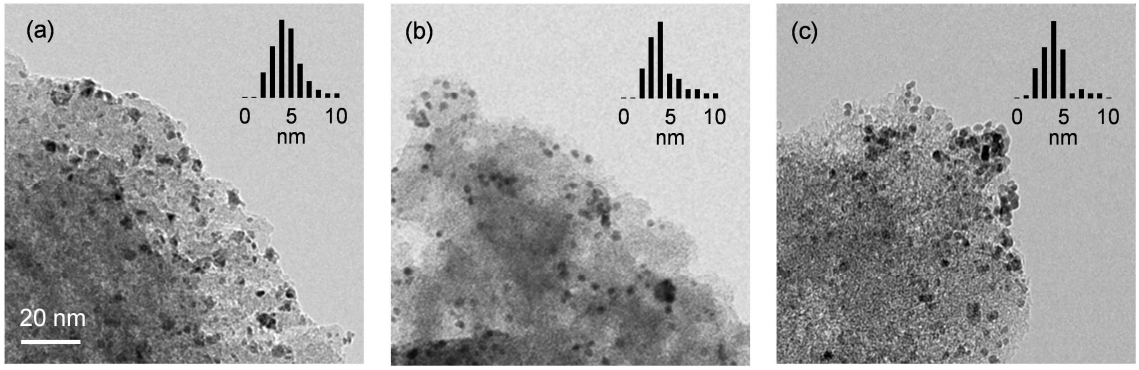

Figure 1. TEM of (a) Pd-HHDMA$_3$/C, (b) fresh and (c) used Pd-HHDMA$_5$/C. The inset shows the particle size distributions and the scale bar applies to all the micrographs.

Table 1. Characterization data of the Pd catalysts.

Catalyst	Pd[a] wt%	HHDMA/Pd[a] mol mol^{-1}	N[b] wt%	D_{CO}[c] %
Pd/C	1.0	0.0	0.0	5
Pd-HHDMA$_1$/C	0.7	0.7	0.1	12
Pd-HHDMA$_2$/C	0.8	1.0	0.2	13
Pd-HHDMA$_3$/C	0.6	4.3	0.3	12
Pd-HHDMA$_4$/C	0.5	8.2	0.4	13
Pd-HHDMA$_5$/C	0.6	11.1	0.7	10
Pd-HHDMA$_5$/TiS	0.5	8.3	0.5	14

[a] Inductively coupled plasma-optical emission spectroscopy (ICP-OES). [b] Elemental analysis. [c] Pd dispersion by CO pulse chemisorption.

moiety, resulting in particle agglomeration. Herein, we show for the first time the suitability of carbon-supported, hexadecyl-2-hydroxyethyl-dimethyl ammonium dihydrogen phosphate ($C_{20}H_{44}NO_5P$, HHDMA)-capped Pd NPs as catalyst in the direct synthesis of H_2O_2. This material benefits from the non-toxic nature of the ligand and its hybrid structure has been proved stable upon alkyne hydrogenation.[10b] Furthermore, we demonstrate *via* the combination of experimental and computational evidences at the Density Functional Theory (DFT) level the crucial role of the ligand in attaining an efficient catalyst. To this end, a series of Pd catalysts with *ca.* 0.6 wt% metal loading labelled as Pd-HHDMA$_n$/C, where n = 1-5 denotes increasing HHDMA/Pd molar ratios,[12] and a catalyst (1.0 wt% Pd loading) featuring naked NPs prepared by dry impregnation (Pd/C) were evaluated. Additionally, a titanium silicate-supported Pd material (Pd-HHDMA$_5$/TiS) was confronted to its C-supported counterpart to unravel the role of the support. Compositional analysis of the solids (**Table 1**) revealed that both the N content and HHDMA/Pd molar ratio increased from Pd-HHDMA$_1$/C to Pd-HHDMA$_5$/C in line with the higher amount of ligand used in the preparation. Transmission electron microscopy (TEM) (**Figure 1**) showed that the Pd NPs possessed a uniform spherical shape with an average diameter of around 4 nm. Despite they were unevenly distributed over the carbon support, no evidence of particle agglomeration was observed, which is related to the function of the ligand moiety in separating the metal phase during the synthesis. Indeed, examination of the Pd dispersion (**Table 1**) revealed similar values for all the HHDMA-modified samples,[13] which was higher than that attained *via* conventional impregnation (Pd/C).

Assessment of the catalytic response of the Pd/C catalyst in the direct synthesis of H_2O_2 displayed comparable results to those previously reported for these materials.[6] Upon an increase of the HHDMA ligand content (**Figure 2a**), augmented H_2O_2 productivity as well as selectivity to H_2O_2 was observed. In line with its highest ligand content, Pd-HHDMA$_5$/C exhibited the

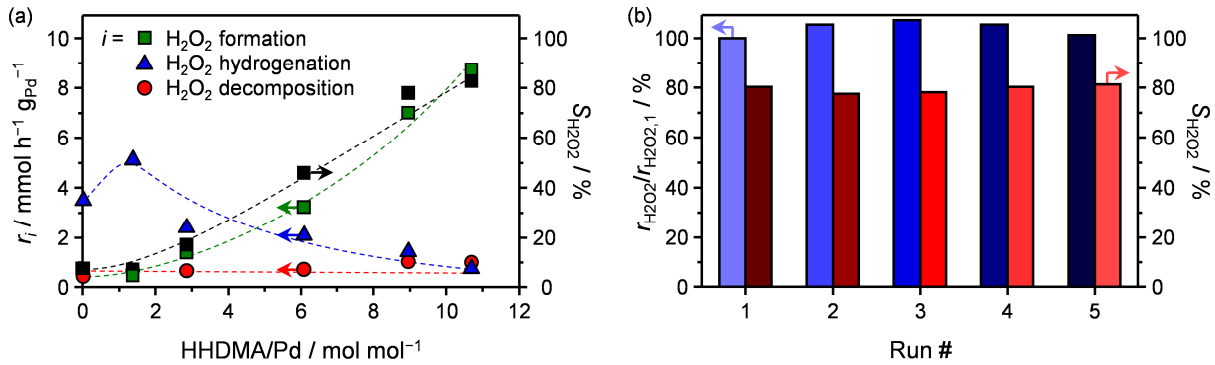

Figure 2. (a) Effect of the HHDMA/Pd molar ratio on the rates of H_2O_2 formation, decomposition, and hydrogenation and on the H_2O_2 selectivity. (b) Fraction of the initial activity and H_2O_2 selectivity over Pd-HHDMA$_5$/C upon 5 consecutive runs. Conditions: T = 273 K, P = 40 bar, 3.75 vol% H_2; 7.50 vol% O_2; 88.75 vol% N_2, m_{cat} = 10 mg in 5 cm^3 of 67 vol% methanol in water.

highest productivity (8.4 mol_{H2O2} h^{-1} g_{Pd}^{-1}) and selectivity (80%), surpassing most of the state-of-the-art materials (**Table 2**). The H_2O_2 selectivity was comparable to that attained for the bimetallic AuPd system but lower than that recently reported for SnPd alloys supported on TiO_2. Furthermore, the H_2O_2 hydrogenation activity was hindered upon increased amount of HHDMA and was negligible for the best-performing Pd-HHDMA$_5$/C catalyst. Additional H_2O_2 decomposition experiments showed that the rate of this reaction did not depend on the ligand content neither on the carbon support, despite a different C support was used for the industrial preparation of Pd-HHDMA$_5$/C.Accordingly, similar results were attained upon evaluation of the sole activated carbon (**Table S1**). The key influence of the support on this transformation was confirmed by the high decomposition rates observed over the bare TiS, which limited the productivity of Pd-HHDMA$_5$/TiS to 0.3 mol_{H2O2} h^{-1} g_{Pd}^{-1}. Finally, the stability of the Pd-HHDMA$_5$/C catalyst was evaluated by monitoring the performance over 5 consecutive runs (**Figure 2b**), revealing that both the productivity and selectivity to H_2O_2 were maintained. Additional characterization of the used catalyst showed that, in contrasts to previous reports,[11b] the morphology of the Pd NPs was fully preserved (**Figure 1c**) and no leaching of Pd or ligand was observed upon ICP-OES analysis of the reaction mixtures.

DFT calculations performed over Pd(111) and Pd(111)-HHDMA surfaces enabled to resolve the key role of the ligand at the molecular scale. The complex structure of the hybrid surface has been disclosed previously, and was shown to comprise strongly adsorbed $H_2PO_4^-$ groups, whose charge is compensated by the ammonium headgroups of the organic surfactant.[10b] The direct synthesis of H_2O_2 proceeds *via* O_2 adsorption followed by two subsequent hydrogenation steps leading to an hydroperoxyl (OOH) and to H_2O_2. Overall, the activation energy for this path is lower on the naked (0.74 eV, 1 eV = 96 kJ mol^{-1}) than on the hybrid Pd surface (1.18 eV, **Table S2**). Nevertheless, the different selectivity observed experimentally can be explained considering the activation barriers for the selective and unselective transformations of the OOH intermediate (**Figure 3** and **Table S2**). The overhydrogenation and decomposition pathways are favored over Pd(111) compared to the formation of H_2O_2 (**Figure S1**). In contrast, on the Pd(111)-HHDMA surface, not only the hydrogenation of the adsorbed OOH intermediate to H_2O_2 is preferred *versus* the overhydrogenation to water, but also the desorption of the product is energetically

Table 2. Comparison of the performance of the Pd-HHDMA$_5$/C catalyst with state-of-the-art materials.

Catalyst	Pd wt%	Ligand	S_{H2O2} %	$r_{H2O2\ formation}$ mol_{H2O2} h^{-1} g_{Pd}^{-1}	Ref.
Pd-HHDMA$_5$/C	0.6	HHDMA	80	8.4	This work
Pd/C nanofibers	1.0	PVA	n.a.	0.6	13
Pd/N-doped C	0.9	PVA	45	14.2[a]	11a
Pd/C	5.0	none	n.a.	2.7	6
AuPd/C	2.5	none	80	4.4	8b
SnPd/TiO_2	3.0	none	96	2.0	8c

[a] H_2SO_4 was added to the reaction medium as promoter.

advantageous over its further hydrogenation and/or decomposition. Notably, the presence of the ligand increases the activation energy of the two side reactions. Furthermore, water formation attributed to O_2 dissociation is only feasible on the naked Pd surface, while it is thermodynamically impeded on the Pd(111)-HHDMA surface (**Table S3**). Other hydrogenation pathways, involving the protonation of adsorbed species due to interfacial acidity,[14] are likely not taking place if the low energy barriers for H_2 dissociation and OOH formation are considered.

The differences in the energy profiles between the naked and the hybrid Pd NPs arises from the adsorption configuration of O_2 and the hydroperoxyl radical. These intermediates flatten on the Pd(111) surface (**Figure 3** and **S2**), thus favoring the cleavage of the O-O bond. In contrast, on Pd(111)-HHDMA, the electrostatic interaction of the adsorbed intermediates with the $H_2PO_4^-$ group and the quaternary ammonium headgroups of HHDMA molecule enables the peculiar vertical configuration of the intermediate, impeding the cleavage of the O-O bond and its overhydrogenation. This is reflected by the decrease of the average atomic O-N distance from 6.64 to 5.95 Å between the horizontal and the vertical adsorption (**Figure S3**). Such a ligand-imposed adsorption geometry resembles that observed at the active site of metalloenzymes, where the allowed reaction paths are determined by the directionality of the interaction between the substrate, the metal center, and the amino acid residues in the surroundings. Whether this behavior is unique to the HHDMA ligand clearly merits further exploration, especially as the interests in the role of electric fields in boosting selectivity is growing.[15] Finally, it should be noted that, apart from the

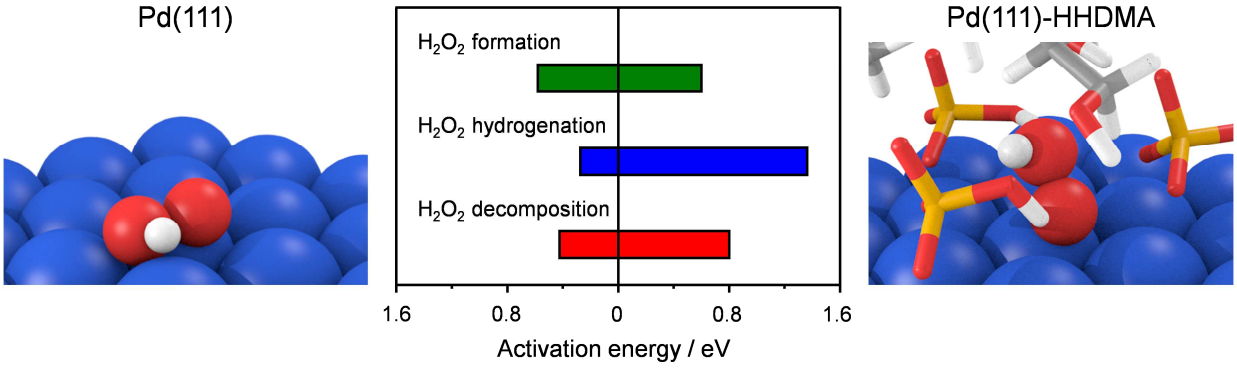

Figure 3. Activation energies for the direct synthesis of H_2O_2 and the side reactions leading to water formation *via* H_2O_2 hydrogenation and decomposition. The drawings represent the adsorption configuration of the hydroperoxyl (OOH) radical on Pd(111) and Pd(111)-HHDMA surfaces.

molecular reorientation on ligand-decorated structures, previously proposed as selectivity descriptors,[10e] steric hindrance caused by the presence of the ligand can also contribute to the observed selectivity patterns as observed on earlier studies with bulkier molecules.[10b] However, the small size of the molecules involved in this case results in a negligible impact of the ensemble confinement on the selective performance.

In conclusion, we have shown the outstanding activity, selectivity, and stability of carbon-supported HHDMA-capped Pd NPs in the direct synthesis of H_2O_2. Their performance was correlated with the amount of HHDMA ligand on the surface of the metal. DFT attributed this behavior to the adsorption mode of the reaction intermediates, deriving from their electrostatic interactions with the surfactant. The attained results not only demonstrate the applicability of hybrid materials for the direct synthesis of H_2O_2 but also highlight the importance of understanding the molecular role of the organic ligand for the design of novel nanocatalysts.

Experimental Section

Pd-HHDMA$_n$/C (n = 1-4) catalysts were prepared by immobilization onto activated carbon of colloids obtained using Na_2PdCl_4 as Pd precursor and varying amounts of HHDMA as stabilizing and reducing agent following the experimental protocol described elsewere.[16] Pd-HHDMA$_5$/C (NanoSelect LF 100^{TM}) and Pd-HHDMA$_5$/TiS (NanoSelect LF 200^{TM}), prepared industrially over unspecified carbon and titanium silicate supports following a similar procedure, were used as received. Pd/C was prepared by dry impregnation of activated carbon using Na_2PdCl_4 as the metal precursor. The compositional and structural properties were studied by ICP-OES, elemental analysis, CO pulse chemisorption, and TEM measurements. Direct synthesis of H_2O_2 was conducted in a batch reactor at 273 K and a total pressure of 40 bar (3.75 vol% H_2; 7.50 vol% O_2; 88.75 vol% N_2) using a 67 vol% methanol/water mixture as solvent and 10 mg of catalyst. H_2O_2 (60 mM in 67 vol% methanol/water) hydrogenation and decomposition experiments were performed at 40 bar under 3.75 vol% H_2/N_2 or N_2 atmosphere, respectively. The reaction mixture was stirred for 30 min and the H_2O_2 formed was quantified by titration with $KMnO_4$. The stability of Pd-HHDMA$_5$/C was assessed upon 5 consecutive catalytic runs. DFT calculations were conducted with the Vienna ab initio Simulation Package (VASP),[17] using the RPBE functional and a kinetic cut-off energy of 450 eV. The Pd(111) slabs were constructed with five atomic layers which were periodically repeated and separated by a vacuum gap of 15 Å. The surface contained four adsorbed HHDMA molecules, whose alkyl chain has been shortened to lighten the calculations. The optimization thresholds were 10^{-5} eV and 0.001 eV Å^{-1} for electronic and ionic relaxations, respectively. Further details on catalyst preparation, characterization, testing, and DFT simulations are given in the Supporting Information.

Acknowledgements

This work was funded by the Swiss National Science Foundation (Project Number 200020-159760), the MINECO (CTQ2015-68770-R) and Marie Curie - COFUND (291787-ICIQ-IPMP, M.S.). The Scientific Center for Optical and Electron Microscopy at ETH Zurich, ScopeM, is acknowledged for the use of its facilities. Dr. S. Mitchell is thanked for the TEM measurements.

Keywords: colloidal synthesis • density functional calculations • peroxides • ligand-stabilized palladium nanoparticles • hybrid catalysts

[1] Y. Yi, L. Wang, G. Li, H. Guo, *Catal. Sci. Technol.* **2016**, *6*, 1593-1610.
[2] "Hydrogen Peroxide Market - Global Industry Analysis, Size, Share, Growth, Trends and Forecast, 2015 - 2023", can be found under https://globenewswire.com/.
[3] J. García-Serna, T. Moreno, P. Biasi, M. J. Cocero, J.-P. Mikkola, T. O. Salmi, *Green Chem.* **2014**, *16*, 2320-2343.
[4] J. M. Campos-Martin, G. Blanco-Brieva, J. L. G. Fierro, *Angew. Chem.* **2006**, *118*, 7116-7139; *Angew. Chem. Int. Ed.* **2006**, *45*, 6962-6984.
[5] a) Q. Chen, E. J. Beckman, *Green Chem.* **2008**, *10*, 934-938; b) S. Shibata, T. Suenobu, S. Fukuzumi, *Angew. Chem.* **2013**, *125*, 12553-12557; *Angew. Chem. Int. Ed.* **2013**, *52*, 12327-12331; c) S. Fukuzumi, *Biochim. Biophys. Acta, Bioenerg.* **2016**, *1857*, 604-611.
[6] E. N. Ntainjua, J. K. Edwards, A. F. Carley, J. A. López-Sánchez, J. A. Moulijn, A. A. Herzing, C. J. Kiely, G. J. Hutchings, *Green Chem.* **2008**, *10*, 1162-1169.
[7] A. Plauck, E. E. Stangland, J. A. Dumesic, M. Mavrikakis, *Proc. Natl. Acad. Sci. U. S. A.* **2016**, *113*, E1973-E1982.
[8] a) J. K. Edwards, J. Pritchard, L. Lu, M. Piccinini, G. Shaw, A. F. Carley, D. J. Morgan, C. J. Kiely, G. J. Hutchings, *Angew. Chem.* **2014**, *126*, 2413-2416; *Angew. Chem. Int. Ed.* **2014**, *53*, 2381-2384; b) J. K. Edwards, B. Solsona, E. Ntainjua, A. F. Carley, A. A. Herzing, C. J. Kiely, G. J. Hutchings, *Science* **2009**, *323*, 1037-1041; c) S. J. Freakley, Q. He, J. H. Harrhy, L. Lu, D. A. Crole, D. J. Morgan, E. N. Ntainjua, J. K. Edwards, A. F. Carley, A. Y. Borisevich, C. J. Kiely, G. J. Hutchings, *Science* **2016**, *351*, 965-968; d) M. García-Mota, N. López, *Phys. Chem. Chem. Phys.* **2011**, *13*, 5790-5797; e) J. Li, T. Ishihara, K. Yoshizawa, *J. Phys. Chem. C* **2011**, *115*, 25359-25367; f) J. Li, K. Yoshizawa, *Catal. Today*, **2015**, *248*, 142-148.
[9] C.-J. Jia, F. Schüth, *Phys. Chem. Chem. Phys.* **2011**, *13*, 2457-2487.
[10] a) T. Bürgi, A. Baiker, *Acc. Chem. Res.* **2004**, *37*, 909-917; b) G. Vilé, N. Almora-Barrios, S. Mitchell, N. López, J. Pérez-Ramírez, *Chem. - Eur. J.* **2014**, *20*, 5926-5937; c) T. Taguki, K. Isozaki, K. Miki, *Adv. Mater.* **2012**, *24*, 6462-6467; d) Z. Niu, Y. Li, *Chem Mater.* **2014**, *26*, 72-83; e) S. T. Marshall, M. O'Brien, B. Oetter, A. Corpuz, R. M. Richards, D. K. Schwartz, J. W. Medlin, *Nat. Mater.* **2010**, *9*, 853-858; f) G. Chen, C. Xu, X. Huang, J. Ye, L. Gu, G. Li, Z. Tang, B. Wu, H. Yang, Z. Zhao, Z. Zhou, G. Fu, N. Zheng, *Nat. Mater.* **2016**, *15*, 564-569.
[11] a) S. Abate, R. Arrigo, M. E. Schuster, S. Perathoner, G. Centi, A. Villa, D. Sub, R. Schlögl, *Catal. Today* **2010**, *157*, 280-285; b) S. Abate, M. Freni, R. Arrigo, M. E. Schuster, S. Perathoner, G. Centi, *ChemCatChem* **2013**, *5*, 1899-1905.
[12] P. T. Witte, P. H. Berben, S. Boland, E. H. Boymans, D. Vogt, J. W. Geus, J. G. Donkervoort, *Top. Catal.* **2012**, *55*, 505-511.
[13] A. Villa, S. J. Freakley, M. Schiavoni, J. K. Edwards, C. Hammond, G. M. Veith, W. Wang, D. Wang, L. Prati, N. Dimitratos, G. J. Hutchings, *Catal. Sci. Technol.* **2016**, *6*, 694-697.
[14] D. Albani, Q. Li, G. Vilé, S. Mitchell, N. Almora-Barrios, P.T. Witte, N. López, J. Pérez-Ramírez, *Green Chem.* **2016**, DOI:10.1039/C6GC02586B.
[15] S. Shaik, D. Mandal, R. Ramanan, *Nat. Chem.* **2016**, *8*, 1091-1098.
[16] a) P. T. Witte, P. H. Berben, S. Boland, E. H. Boymans, D. Vogt, J. W. Geus, J. G. Donkervoort, *Top. Catal.* **2012**, *55*, 505-511; b) P. T. Witte, WO2009096783 A1, **2009**.
[17] G. Kresse, J. Furthmüller, *Phys. Rev. B* **1996**, *54*, 11169-11186.

WILEY-VCH

Entry for the Table of Contents

COMMUNICATION

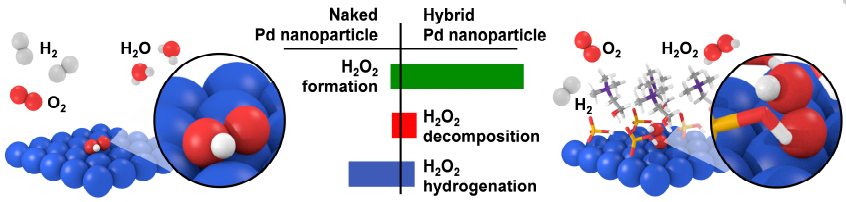

In the ligand we trust: hybrid palladium nanoparticles are selective and stable catalysts for direct H_2O_2 synthesis. The ligand stabilizes the hydroperoxyl intermediate in a vertical configuration preventing side reactions (dissociation and overhydrogenation) compared to naked metal nanoparticles, where flat intermediates are readily converted to water.

*Giacomo M. Lari, Begoña Puértolas, Masoud Shahrokhi, Núria López, and Javier Pérez-Ramírez**

Page 1 – Page 4

Hybrid Palladium Nanoparticles for Direct H_2O_2 Synthesis: the Key Role of the Ligand